

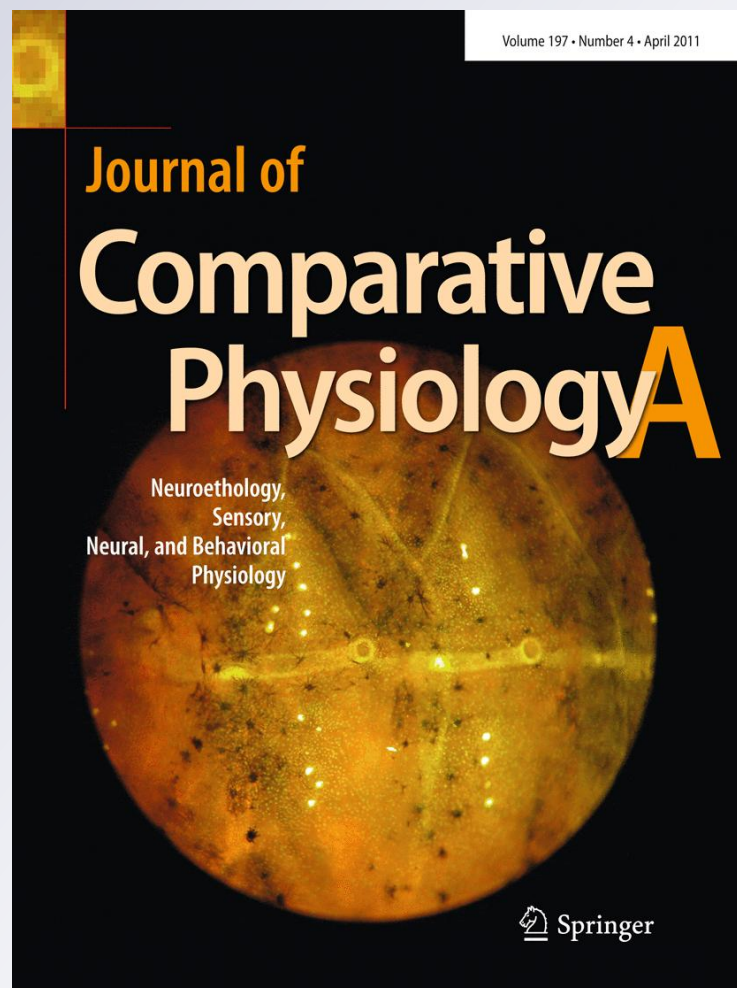
*Variation in the determinants of power
of chemically skinned type I rat soleus
muscle fibres*

**Journal of Comparative
Physiology A**

Neuroethology, Sensory,
Neural, and Behavioral
Physiology

ISSN 0340-7594
Volume 197
Number 4

J Comp Physiol A (2011)
197:311-319
DOI 10.1007/
s00359-010-0613-6



Your article is protected by copyright and all rights are held exclusively by Springer-Verlag. This e-offprint is for personal use only and shall not be self-archived in electronic repositories. If you wish to self-archive your work, please use the accepted author's version for posting to your own website or your institution's repository. You may further deposit the accepted author's version on a funder's repository at a funder's request, provided it is not made publicly available until 12 months after publication.

Variation in the determinants of power of chemically skinned type I rat soleus muscle fibres

Sally F. Gilliver · David A. Jones · Jörn Rittweger · Hans Degens

Received: 17 September 2010/Revised: 9 November 2010/Accepted: 11 November 2010/Published online: 1 December 2010
© Springer-Verlag 2010

Abstract We explored to which extent maximal velocity of shortening (V_{\max}), force per cross-sectional area (specific tension, P_o) and curvature of the force–velocity relationship (a/P_o in the Hill equation) contribute to differences in peak power of single, chemically skinned rat type I fibres. Force–velocity relationships were determined from isotonic contractions of 94 maximally activated fibres. Peak power (\pm SD) was $3.50 \pm 1.64 \text{ W L}^{-1}$. There was a tenfold range of peak power and five-, six- and fourfold ranges for P_o , V_{\max} and a/P_o , respectively. None of the differences between fibres was explicable by differences in myosin heavy or light chain composition. The inverse relationship between a/P_o and V_{\max} suggests a similar underlying cause. Fitting the data to the Huxley (Progr Biophys Biophys Chem 7:255–318, 1957) cross-bridge model showed that the rate constant g_2 and the sum of the rate constants ($f + g_1$) co-varied, both being low in the slowest fibres. Approximately 16% of the variation in P_o could be explained by variation in the proportion of attached cycling cross-bridges ($f/(f + g_1)$), but the origin of most of the variance in P_o remains unknown.

Keywords Skeletal muscle · Skinned fibres · Power · Force–velocity relationship

Abbreviations

a/P_o	Indication of curvature of the force–velocity relationship
CSA	Cross-sectional area
EGTA	Ethylene glycol tetra-acetic acid
f	Rate constant of cross-bridge attachment
g_1	Rate constant of cross-bridge detachment within the positive working range
g_2	Rate constant for cross-bridge detachment once the cross-bridge has passed the neutral position and begins to oppose shortening
M	Fraction maximal force or shortening velocity at which peak power is generated
MHC	Myosin heavy chain
MLC	Myosin light chain
P_o	Specific tension, or force per fibre cross-sectional area
SDS-PAGE	Sodium dodecyl sulfate polyacrylamide gel electrophoresis
V_{\max}	Maximal velocity of shortening
V_{opt}	Shortening velocity at which maximal power is produced

Introduction

Mammalian motor units are generally divided into three or four “types” based on the histochemical and contractile properties of the constituent muscle fibres. However, even in the first descriptions of motor units, it is evident that within each motor unit type there is a considerable range of contractile properties and an overlap between the different types (Burke et al. 1971, 1973). The development of

S. F. Gilliver · D. A. Jones · J. Rittweger · H. Degens (✉)
Institute for Biomedical Research into Human Movement and Health, Manchester Metropolitan University, John Dalton Building, Oxford Road, Manchester M5 1GD, UK
e-mail: h.degens@mmu.ac.uk

J. Rittweger
Department for Space Physiology, Institute of Aerospace Medicine, German Aerospace Center (DLR), Linder Höhe, 51147 Cologne, Germany

techniques to determine the contractile characteristics of single muscle fibre fragments has shown that what is true at the level of the whole motor unit also applies to single fibres. While type I and the various subdivisions of the type II fibres, differentiated on the basis of their myosin heavy chain (MHC) composition, have, on average, different speeds of contraction, there is also considerable variation among fibres of the same type (Larsson and Moss 1993; Bottinelli et al. 1994; Degens and Larsson 2007; Gilliver et al. 2009). The differences between the major classifications of fibres, type I, IIA, IIX, etc., are largely attributed to differences in the properties of the MHCs, but the reason why fibres with the same MHC composition should differ remains to be determined, as does the physiological significance of this variation.

Previous work concerning variation in contractile speed of single muscle fibres of the same type has been concerned with the role of the light chains and, in particular, the content of MLC3 (Bottinelli et al. 1994, 1996). However, the slow type I fibres are reported to be homogeneous with respect to light chain composition and do not express MLC3 (Schiaffino and Reggiani 1996; Degens et al. 1998; Andrucho et al. 2006) but still show considerable variation in contractile properties (Degens et al. 1998; Gilliver et al. 2009). Consequently, it is of interest to understand how variation in other proteins can influence the contractile properties of single fibres that apparently have the same MHC composition.

It is clear from our previous observations of human fibres (Gilliver et al. 2009) that differences in power can arise as a result of variation in any or all of the three factors that contribute to peak power, namely the maximum speed of shortening (V_{\max}), the specific tension (force per unit cross-sectional area, P_0) and the shape of the force–velocity relationship (a/P_0 in the Hill equation). However, it seems unlikely that there will be three separate causes for the variation in power and we have previously presented some preliminary evidence derived from human fibres to suggest that differences in V_{\max} and a/P_0 are linked, there being an inverse relationship between the two (Gilliver et al. 2009).

There are, however, difficulties working with human fibres in that the participants from whom they were derived tend to be of mixed genetic, nutritional and exercise backgrounds. Consequently, single fibres from rat soleus muscle have been used in the work described here with the purpose of determining whether the variation seen with human fibres is evident in rat muscle fibres. Secondly, we aimed to define more precisely the relationship between V_{\max} and a/P_0 . Following on from this second objective, the data have been analysed using the Huxley (1957) model of cross-bridge interaction to obtain some insight into the possible kinetic basis of the relationship between V_{\max} and curvature of the force–velocity relationship.

Methods

Rat muscle

Muscle samples were obtained from adult male Wistar rats (*Rattus norvegicus*) within 10 min after killing. The rats were anaesthetised with pentobarbital (i.p. 50 mg kg⁻¹) and the soleus muscles excised, after which the animals were killed with an overdose of anaesthetic. The animals were used in research projects of other investigators or were control animals in a study on the effect of a vitamin D analogue on skeletal muscle function, all approved by the local animal research ethics committees of the University of Manchester and Vrije Universiteit Amsterdam. The muscles were sampled after the animals had been killed in the course of those studies. Therefore, there is no specific approval for the present study. This is in accord with the generally accepted guideline of reducing animal numbers to a minimum in biomedical research.

Solutions

The solutions have been described previously (Larsson and Moss 1993; Degens et al. 1998; Gilliver et al. 2009). All concentrations are given as mmol L⁻¹. Relaxing solution: MgATP, 4.5; free Mg²⁺, 1; imidazole, 10; EGTA, 2; KCl, 100; with the pH set to 7.0 using KOH. Low EGTA solution was the same as the relaxing solution except that EGTA was 0.5 mM. The pCa ($-\log[\text{free Ca}^{2+}]$) of the activating solution was 4.5 and contained MgATP, 5.3; free Mg²⁺, 1; imidazole, 20; EGTA, 7; creatine phosphate, 19.6; KCl, 64; pH 7.0.

Preparation of muscle samples

The procedures for preparing single fibres and determining their contractile properties were as described by Gilliver et al. (2009) for human fibres and were similar to those used by others (Larsson and Moss 1993). Briefly, small bundles were cut from each muscle and immersed in glycerol/relax at 4°C for 24 h. They were then sucrose-treated, frozen in liquid nitrogen, and stored at -80°C for later use. Sucrose acts as an effective cryoprotectant, and provided bundles are treated with increasing concentrations of sucrose, no damage to contractile function is evident (Frontera and Larsson 1997).

Preparation of single fibres

Fibre bundles were placed in relaxing solution containing 1% Triton X-100 for 20 min to permeabilize the membranes and sarcoplasmic reticulum. Dissecting and

mounting the individual fibres and setting sarcomere length were carried out with the fibre in relaxing solution. Individual fibres (length ≥ 1 mm) dissected from the bundles were mounted in a permeabilized-fibre test system (400, Aurora Scientific Inc., Aurora, ON, Canada) and tied with nylon thread to fine insect pins attached to the force transducer (Aurora, 403A) and motor arm (Aurora, 312C). These were mounted over a moveable stainless steel plate containing a set of machined wells, each with a glass base. The plate was cooled to 15°C and the plate, transducer and motor were mounted on an inverted microscope (Olympus IX71, Tokyo, Japan). The image of the fibre was viewed by a video camera and sarcomere length determined via a Fourier transformation of the sarcomere pattern (900A, Aurora). Sarcomere length was set at 2.6 μm at the start of the experiment and checked at regular intervals thereafter. Fibre diameter was measured at three places while it was suspended in the air and cross-sectional areas calculated assuming that the fibre attained a circular circumference (Degens and Larsson 2007). Fibre length was measured to the nearest 0.01 mm.

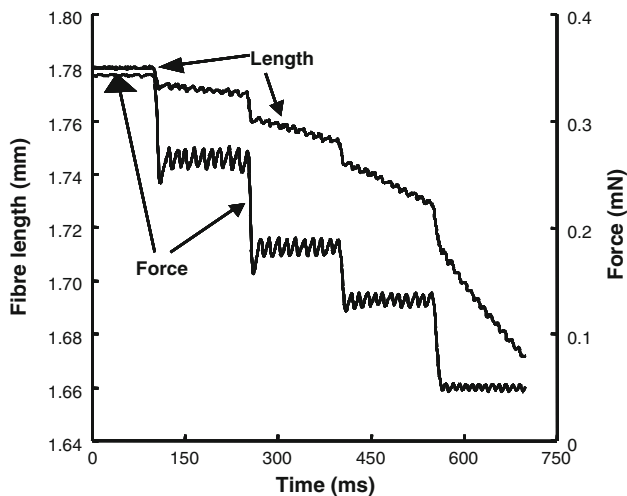


Fig. 1 Length and force signals recorded from a single fibre during a sequence of isotonic shortening steps begun once maximum isometric force had been reached

Contractile properties

Fibres were transferred from the relax solution to a low EGTA solution for 15 s before being moved to the well containing activating solution (pCa 4.5). When the isometric force had reached a plateau, the fibre was subjected to four sequences of four isotonic shortening steps, essentially as described by Bottinelli et al. (1996). In each sequence, the lever arm moved at a speed sufficient to maintain the muscle force at a predetermined percentage of the maximal isometric force (Fig. 1). At the end of the sequence, the fibre was stretched back to its original length while still in activating solution. This sequence was repeated a total of four times at different percentages of isometric force. Each step in a sequence lasted 150 ms (Fig. 1).

Myosin heavy chain and light chain composition of single fibres

After the functional measurements had been completed, the single fibres were dissolved in Laemmli sample buffer, boiled for 2 min and MHCs separated by SDS-PAGE as described before (Larsson and Moss 1993; Degens et al. 1998; Gilliver et al. 2009). MHC type I was clearly separated from the faster myosins (Fig. 2) and only the contractile data from fibres that were unequivocally type I are presented here. Myosin light chain (MLC) composition was determined for a group of fibres with V_{max} at the high or low end of the measured range of values, using 12% SDS-PAGE and the protein bands were identified by comparison with the data of Bottinelli et al. (1996).

Data analysis and statistics

The data for force and length, as shown in Fig. 1, were analysed by fitting least squares linear regressions to the last 100 ms of each step, generating a value for velocity of shortening for a given force and yielding 16 data points for each fibre. These data were fitted to the Hill equation $(P + a)(V + b) = (P_0 + a)b$ (Hill 1938) using a non-

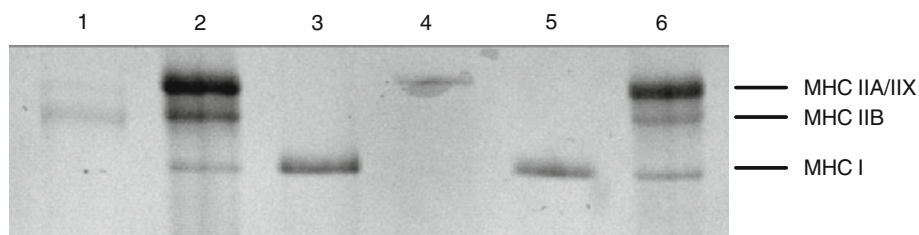


Fig. 2 SDS-PAGE separation of rat MHC. Lanes 2 and 6 were loaded with a whole muscle extract of rat plantaris muscle to act as markers for band identification. Single fibres in lanes 3 and 5 contain

MHC-I. The fibre in lane 4 contains MHC IIA and lane 1 shows a hybrid IIX/IIB fibre; both were excluded from the data analysis

linear least squares regression and an iterative routine written in Matlab (v7.1, The Mathworks Inc., USA) to give best fit values for the Hill constants a and b , with P expressed as a fraction of P_o . These values were then used to estimate the maximum velocity of unloaded shortening (V_{max}) as fibre lengths per second ($FL\ s^{-1}$).

The fraction (M) of P_o or V_{max} at which peak power was generated was calculated as: $M = (\sqrt{1 + G} - 1)/G$, derived from the Hill equation, where G is P_o/a or V_{max}/b (Woledge et al. 1985). Maximum power was calculated as: $M^2 \times P_o \times V_{max}$ and is reported as Watts per litre ($W\ L^{-1}$).

All fibre segments were obtained from different fibres. Data were rejected if the isometric force decreased by more than 10% over the course of the four sequences of isotonic shortening contractions, the sarcomere length had changed by more than $0.1\ \mu m$ or had become heterogeneous, or if R^2 was less than 0.96 when fitting the data to the Hill equation. The reproducibility of the contractile measurements was checked by repeating the series of isotonic shortening and data analyses in 18 fibres. The coefficients of variation for V_{max} , a/P_o and P_o were 6, 10 and 2%, respectively.

In addition, for modelling purposes, force–velocity curves were fitted to the Huxley model (Huxley 1957) such that the force P is given as a fraction of the isometric force, P_o , for velocities of shortening V :

$$P/P_o = 1 - (1 - \exp(-\Phi/V))V/\Phi \times (1 + ((f + g_1)/g_2)^2 V/2\Phi)$$

where f is the rate constant for attachment, g_1 that for detachment within the positive working range of the cross-bridge and g_2 the rate constant for detachment once the cross-bridge has passed the neutral position and begins to oppose shortening. $\Phi = (f + g_1)h$, where h is a constant related to the distance over which a cross-bridge may act and was taken as 0.025. Data were fitted to the equation using a non-linear least squares regression run in Microsoft Excel 2007 using the “Solver” function to obtain values of

$(f + g_1)$ and g_2 . A more rigorous test of goodness of fit was applied and only those fibres where $R^2 > 0.98$ were accepted, see “Results” for details.

Data were tested for normality using the Shapiro–Wilk test and were found not to be normally distributed; the values are reported as means, median and range. The strength of association between observed variables was assessed using Spearman’s rank correlation.

Results

Data from the 94 fibres that contained only type I MHC are included in the analysis presented here. Examples of force–velocity data from three individual fibres are shown in Fig. 3. These three fibres are representative of fibres with low, medium and high peak power production and their positions in the spectrum of contractile properties are indicated in Fig. 4. The median and range of values are given in Table 1. Fibres ‘1’ and ‘2’ in Fig. 3 had similar values of P_o but differed in peak power primarily because of differences in V_{max} , while fibre ‘3’ had the highest peak power of the three with higher values of both P_o and V_{max} . Another factor that determines the power output of a fibre is the curvature of the force–velocity relationship, where higher values of a/P_o indicate a less curved relationship and thus higher peak power. The slowest of these three fibres (1) had a value of a/P_o of 0.34, while that of the fastest (3) was 0.11 indicating that the differences in curvature tended to counteract the influence of differences in V_{max} on peak power.

Figure 4a, b and c shows the relationships between peak power and P_o , V_{max} and a/P_o , respectively. There was about a fivefold range in P_o , a sixfold range in V_{max} and just under a tenfold range in peak power. Curvature of the force–velocity relationship (a/P_o) showed a nearly fourfold range. Peak power was positively related to P_o ($R^2 = 0.70$, $P < 0.001$; Fig. 4a) and V_{max} ($R^2 = 0.52$, $P < 0.001$; Fig. 4b), but negatively to a/P_o ($R^2 = 0.21$, $P < 0.001$;

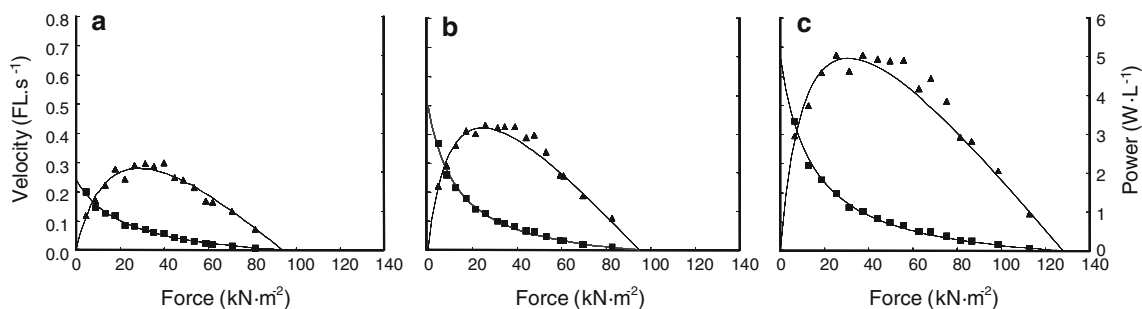


Fig. 3 Data obtained during isotonic shortening contractions from individual type I rat soleus muscle fibres. **a**, **b** and **c** Three fibres with differing contractile properties, referred to in the text and subsequent

figures as fibres ‘1’, ‘2’ and ‘3’. Squares are measures of velocity and triangles of power for a given force. Force–velocity and power curves have been fitted to the data according to the Hill equation

Fig. 4 Peak power of single rat soleus type I muscle fibres as a function of maximum isometric force and shortening velocity. **a** Peak power as a function of maximum isometric force per unit cross-sectional area (P_o). **b** Peak power as a function of the maximum velocity of shortening (V_{max}). **c** Peak power as a function of the curvature of the force–velocity relationship (a/P_o). Data from individual fibres; fibres 1, 2 and 3 are the three fibres illustrated in Fig. 3

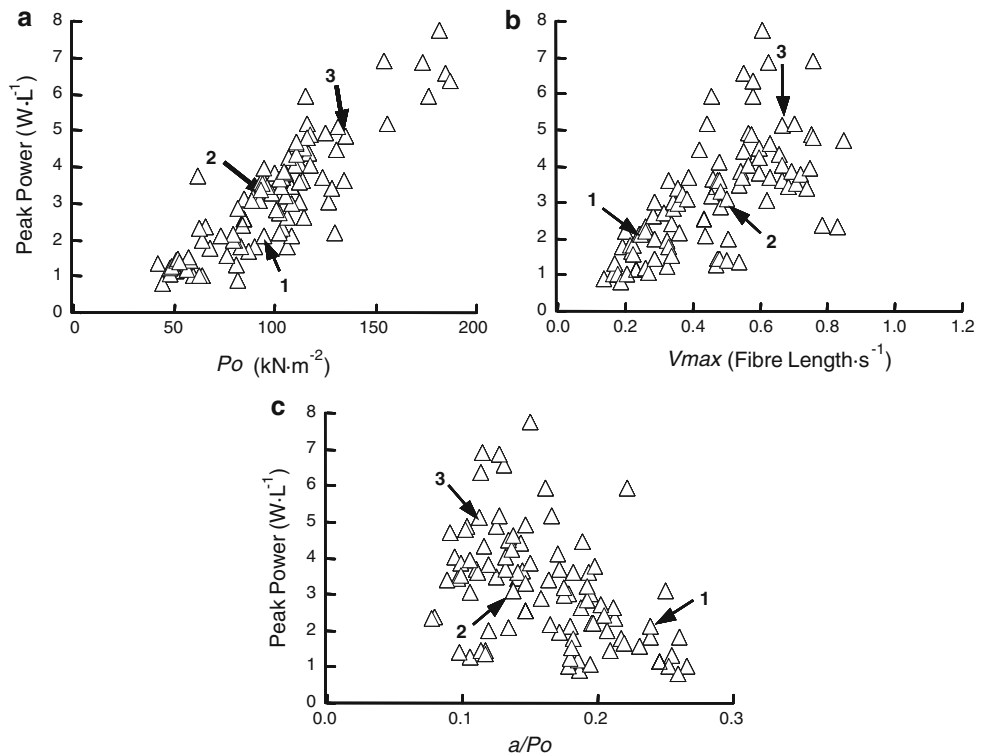


Table 1 Contractile properties of rat type I single muscle fibres ($N = 94$)

	CSA (μm^2)	Force (μN)	P_o (kN m^{-2})	V_{max} (FL s^{-1})	Peak power (W L^{-1})	a/P_o	V_{opt} (FL s^{-1})
Mean	3,744	357	99	0.46	3.16	0.161	0.12
Median	3,579	341	102	0.47	3.09	0.160	0.12
Range	1,521–8,659	112–800	42–187	0.14–0.85	0.81–7.76	0.077–0.266	0.04–0.21

Data are given for fibre cross-sectional area (CSA), maximum isometric force and force per cross-sectional area (P_o). The maximal velocity of shortening (V_{max}), curvature (a/P_o) and the velocity (V_{opt}) at which peak power was generated were estimated by fitting data to the Hill equation

Fig. 4c), where the highest values of a/P_o were associated with lower peak powers (see also Table 1).

There was a clear relationship between a/P_o and V_{max} (Fig. 5) such that a/P_o decreased with increasing V_{max} .

While only type I MHC fibres were used it remains possible that the faster fibres may have expressed some faster MLC isoforms. This was checked by separating the protein extracts on 12% gels (Fig. 6). It is evident that the same pattern of bands was present in fibres with very different maximum velocities of shortening and that none of the type I fibres expressed MLC3 or the fast isoforms of MLC1 or MLC2.

Fitting the data to the Huxley equation proved to be more difficult than to the Hill equation as, despite a good fit ($R^2 > 0.96$), estimated values of V_{max} and power were sometimes clearly unrealistic. Figure 7 presents the data

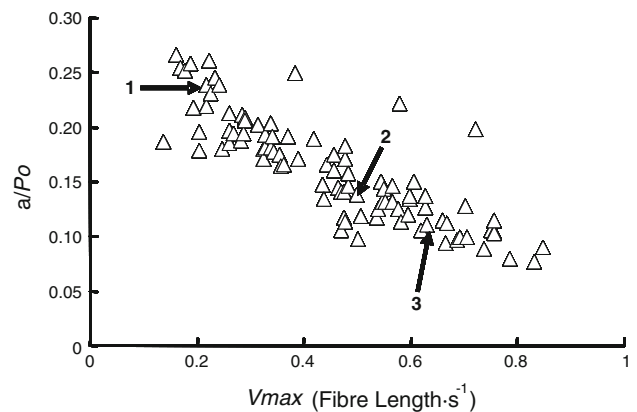


Fig. 5 The relationship between curvature of the force–velocity relationship (a/P_o) and maximum velocity of shortening (V_{max}) for rat soleus type I fibres

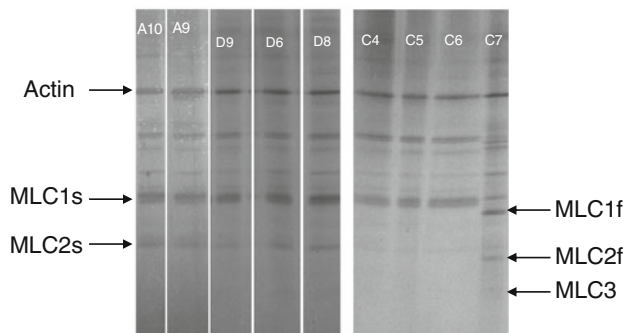


Fig. 6 Light chain composition of single fibres. On the *left*, five type I fibres arranged in order of increasing V_{max} , A10, 0.31 FL s^{-1} ; A9, 0.32 FL s^{-1} ; D9, 0.74 FL s^{-1} ; D6, 0.81 FL s^{-1} ; D8, 0.89 FL s^{-1} . On the *right*, three type I fibres (C4, 5 and 6) compared with one type IIA fibre (C7). V_{max} for these four fibres were: C4, 0.86 FL s^{-1} ; C5, 0.26 FL s^{-1} ; C6, 0.29 FL s^{-1} ; C7, 1.03 FL s^{-1}

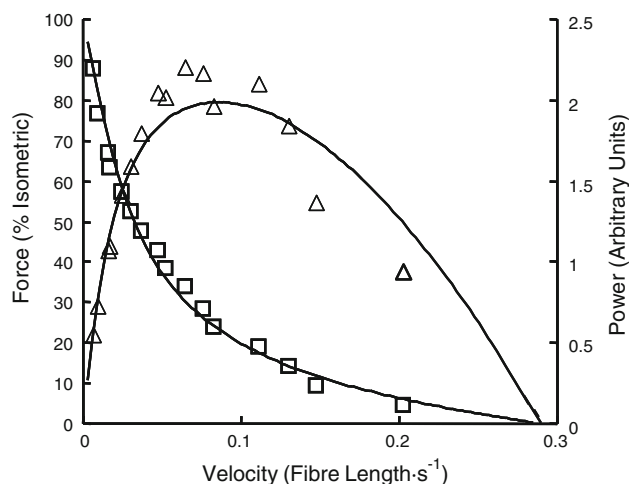


Fig. 7 Single fibre data fitted to the Huxley cross-bridge model. Rate constants $(f + g_1) = 2.11$, $g_2 = 11.4$. The value R^2 for the fit to the force–velocity curve was 0.985

for one fibre that shows a typical pattern with the data points falling just below the power curve at high forces and above the curve at intermediate forces so that the actual peak power was slightly larger and earlier than predicted by the fitted curve. Where the R^2 value fell below 0.98 the discrepancy became marked; the fibre shown in Fig. 7 was on the borderline of acceptance. Consequently, the analysis is restricted to the 68 fibres where there was a good and realistic fit to the data. These 68 fibres were representative of the larger population (as can be seen from comparable values in Tables 1, 2). The values for peak power and the spread of data were virtually identical using the two methods (Table 2). There was a tight correlation between the estimates of V_{max} from the Hill and Huxley equations but with those from the Huxley model being slightly higher for the slower fibres and lower for the faster fibres (see the ranges of V_{max} in Table 2).

Table 2 Comparison of values obtained for the force–velocity relationship using the Hill and Huxley equations

	Peak power (W L^{-1})	Po (kN m^{-2})	V_{max} (FL s^{-1})	a/Po
Hill				
Mean	3.12	95	0.48	0.15
SD	1.53	33	0.17	0.05
Median	3.12	94	0.48	0.14
Max	6.89	187	0.85	0.25
Min	1.00	42	0.17	0.08
	Peak power (W L^{-1})	Po (kN m^{-2})	V_{max} (FL s^{-1})	$(f + g)/g_2$
Huxley				
Mean	3.15	95	0.43	0.21
SD	1.58	33	0.13	0.03
Median	3.12	94	0.43	0.21
Max	7.06	187	0.67	0.26
Min	0.96	42	0.19	0.14

Values obtained for the 68 fibres where the Huxley equation provided a good fit to the data (see text). Po is the measured value for isometric force and is the same for both methods; curvature is given as a/Po for the Hill equation and $(f + g_1)/g_2$ for the Huxley equation

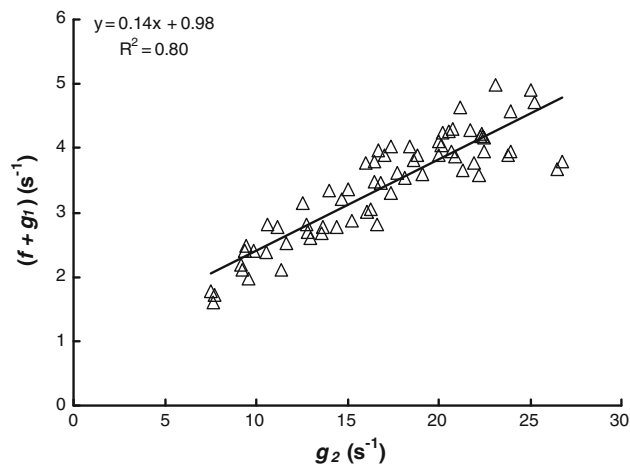


Fig. 8 The relationship between the rate constants g_2 and $(f + g_1)$. The rate constants were estimated by fitting the force–velocity data for individual fibres to the Huxley model

The relationship between the rate constants $(f + g_1)$ and g_2 is shown in Fig. 8. The sum of the rate constants $(f + g_1)$ declined in a linear fashion as the fibres slowed (lower values of g_2) but with an intercept on the ordinate of approximately 1.0 s^{-1} . As a consequence of this intercept, the values of $(f + g_1)/g_2$ were higher for the slower fibres (Fig. 9). The ratio $(f + g_1)/g_2$ is the equivalent of a/Po in the Hill equation and is a measure of the curvature of the force–velocity relationship with high values indicating a

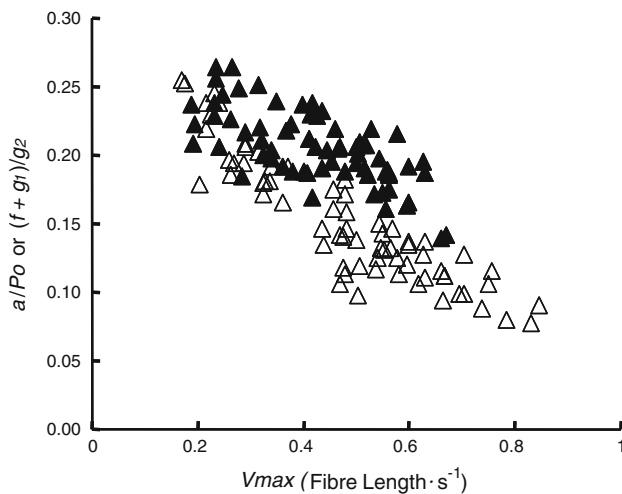


Fig. 9 The relationship between curvature of the force velocity relationship and maximum velocity of shortening (V_{max}) for individual fibres. *Open symbols* Points derived from fitting the data to the Hill equation (as in Fig. 5). *Filled symbols* Points derived from fitting the data to the Huxley model

flatter curve. Values of a/Po and $(f + g_1)/g_2$ were similar for the slow fibres and both decreased as the fibres became faster, although the range of values for $(f + g_1)/g_2$ was not as great as that for a/Po (Fig. 9; Table 2).

Discussion

The results presented here have allowed a detailed examination of the reasons underlying the variations in power seen in single muscle fibres of the same “type”, based on their MHC composition. Our findings confirm previous observations on human fibres (Gilliver et al. 2009) that there is considerable variation in the three factors that determine power, namely the specific tension, Po ; the maximum velocity of shortening, V_{max} ; and the curvature of the force–velocity relationship. Furthermore, the results confirm the observation that there is an inverse relationship between curvature and V_{max} such that with faster fibres the curvature was greater.

A concern when dealing with single fibre fragments is that the variation seen may have been as a consequence of damage. For this reason care was taken to restrict analysis to fibres that maintained isometric force within 10% of the initial value during the sequence of isotonic shortenings, where sarcomere length changed by $\leq 0.1 \mu\text{m}$ and where the curve fitting by least square regression gave R^2 values ≥ 0.96 . Values for specific tension (mean 105 kN m^{-2} ; Table 1) are similar to reports of Thompson and Brown (1999) and Husom et al. (2005) and the variance in Po of 31% is similar to that reported by others of around 35% (Bottinelli et al. 1994; Thompson and Brown 1999;

Degens and Larsson 2007). Part of the variability may be related to difficulties in measuring the cross-sectional area since fibres are rarely circular and skinned fibres are liable to shrinkage and swelling depending on whether they are measured in air or fluid. We have estimated the cross-sectional area from the diameter of the fibre while it was briefly suspended in air. This has been suggested to give estimates that correspond most closely with cross-sectional areas determined from histological sections (Degens et al. 1999; Degens and Larsson 2007). Interestingly, even the force generating capacity of segments along the length of a given intact fibre may vary by 10% (Edman et al. 1985). Estimates of V_{max} and a/Po are also liable to random experimental error but the coefficients of variation, determined by duplicate measures on single fibres, were insignificant compared to the several-fold variations in contractile properties seen between fibres. Values describing the force–velocity relationship were fitted to the Hill equation and it is evident in Fig. 3 that there was a close correspondence between the fitted curves and the actual data points. The fits were obtained expressing values of force as a percentage of observed Po , thus fixing the intercept of the curve on the ordinate. There is, however, an argument for fitting the curves using the actual forces and allowing the iterative process to fit a value of Po since the force–velocity relationship has been reported to deviate from a true hyperbola at high force values (Edman et al. 1997). Furthermore, determination of V_{max} by extrapolation of the force–velocity relationship to zero load may be somewhat uncertain (Josephson and Edman 1988). Allowing Po to vary gave estimated values which were, on average, 9% higher than the measured values of Po but the range of values for Po , V_{max} and a/Po between the different fibres was similar with both methods.

V_{max} varied sixfold (Table 1) with the bulk of the fibres spanning at least a fourfold range (Fig. 4b). Bottinelli et al. (1991, 1994) have reported around a threefold range in V_{max} at a slightly lower temperature of 12°C , and we have previously reported that the V_o of rat soleus type I fibres, as determined with the slack test, also varied six- to sevenfold (Degens et al. 1998). Even along the length of a given fibre, V_{max} has been shown to vary by as much as 30% (Edman et al. 1985).

V_{max} may be modulated by the MLC composition (Greaser et al. 1988; Sweeney et al. 1988; Bottinelli et al. 1994, 1996). However, separation of the MLCs (Fig. 6) showed no obvious differences in the pattern of bands seen on the gels between fibres of differing V_{max} nor was there any evidence of MLC3 or the fast isoforms of MLC1 and MLC2 in the type I fibres. It is thus unlikely that the large variation in V_{max} in the rat type I fibres in our study is explained by differences in MLC composition.

Differences in a/Po have long been associated with differences in the contractile speed of muscles (Katz 1939; Close 1972; Lännergren 1978) where faster muscles have greater values of a/Po . However, examination of the data from single fibre preparations reveals a more complex picture. Within a species, the faster fibres do have, on average, higher values of a/Po , but there is also appreciable overlap between fibre types in, for instance, rat (Bottinelli et al. 1991) and human fibres (Bottinelli et al. 1996; Gilliver et al. 2009). The curvature of the force–velocity relationship affects the velocity, or force, at which peak power is obtained and this can be determined as the constant M , derived from a/Po , as detailed in “Methods” (Woledge et al. 1985). For two fibres with similar values of Po and V_{max} , a difference in curvature will lead to differences in peak power, the less curved and higher the value of a/Po , the greater the power. The contribution of curvature to peak power, independent of Po and V_{max} , is given by M^2 (Woledge et al. 1985) and the values of M^2 , which ranged from 0.030 to 0.099, indicate a threefold influence of curvature on peak power in the type I fibres measured here.

In our previous examination of variation in power of individual human fibres, we noted a tendency for an inverse relationship between a/Po and V_{max} (Gilliver et al. 2009), which has also been observed in intact frog fibres (Edman et al. 1985). One of the objectives of the present study was to obtain clearer evidence of this in a larger group of type I fibres. The data shown in Fig. 5 clearly confirm the earlier observations with a/Po declining and the force–velocity relationship becoming more curved as V_{max} increases. The effect of this on the peak power is contradictory since while a higher value of V_{max} confers higher power, a greater curvature has the opposite effect as can be seen comparing Fig. 4b and c. The effect is also in contrast to that seen between fast and slow muscles, where curvature of the force–velocity relationship of fast muscle is less than that of slow muscle (Edman 2010).

To obtain some insight into the mechanisms underlying the relationship between curvature and shortening velocity, we analysed the data on the basis of the Huxley model of cross-bridge interaction. The curves did not fit the data as well as with the Hill equation (see Fig. 7 and associated comments in “Results”) but excluding the minority of fibres where there was a poor fit, a positive linear relationship between the sum of the rate constants ($f + g_1$) and g_2 , with an intercept on the ordinate was clear. The value of ($f + g_1$) lies between about 2.0 and 5.0 s^{-1} , and although the Huxley analysis does not give separate values for f and g_1 , it is generally assumed that f has to be greater than g_1 to permit a reasonable proportion of cycling cross-bridges to be attached in the isometric state. If this is the case, then a threefold difference in ($f + g_1$) requires a substantial

variation in f as differences in g_1 would have comparatively little effect. One explanation of the intercept on the ordinate in Fig. 8 is, therefore, that it represents the constant value of g_1 and it is only f that differs with V_{max} . If this is the case and the value of g_1 is approximately 1 s^{-1} , then over the range of values for ($f + g_1$) of 2.0–5.0 s^{-1} , f would have to increase fourfold from 1 to 4 s^{-1} . This is similar to the fourfold range of values found for g_2 in these fibres (Fig. 8).

The relationship between ($f + g_1$) and g_2 shown in Fig. 8 provides an indication of why curvature of the force velocity relationship varies with V_{max} , as shown in Fig. 5. In the Huxley model, the ratio ($f + g_1$)/ g_2 is the equivalent of a/Po in the Hill equation, providing a measure of curvature (Simmons and Jewell 1974). The intercept on the ordinate in Fig. 8 means that when dividing ($f + g_1$) by g_2 the ratio ($f + g_1$)/ g_2 , and thus curvature, is not constant, being relatively high for the slower fibres and decreasing in the fast fibres (Fig. 9). The values for ($f + g_1$)/ g_2 and a/Po diverge for the faster fibres but the values are similar for the slow fibres and the trend to decrease with increasing velocity is common to both (Fig. 9). It appears likely, therefore, that differences between fibres in curvature and maximum velocity of unloaded shortening have a common origin. However, the nature of the difference that would affect both the rate constants f and g_2 in the Huxley model remains to be determined.

The present results show similar variations in Po to that reported for human fibres (Gilliver et al. 2009) and possible explanations were discussed in that paper. As with human fibres, while it is impossible to rule out small admixtures of fast heavy or light chains, these must be small to remain undetected with SDS-PAGE and are unlikely to account for the range of specific tensions that are seen. One possibility that arises from the discussion of the rate constants f and ($f + g_1$) is that variation in f between fibres leads to differences in the proportion of available cross-bridges that are attached and potentially generating force, given by $f/(f + g_1)$. If g_1 is 1.0 s^{-1} and f varies between 1.0 and 4.0 s^{-1} , then $f/(f + g_1)$ will range from 0.5 to 0.8, a 60% increase between the slowest and fastest fibres. Figure 10 plots Po as a function of V_{max} , and the regression line suggests a 50% increase in specific tension over this range, similar to the predicted value. However, the R^2 value of 0.16 indicates that this accounts for less than 20% of the variance in Po .

In summary, previous observations obtained on single human fibres of the same MHC composition of considerable variation in Po , V_{max} and curvature of the force–velocity relationship have been confirmed for rat soleus fibres. The weak association previously observed between curvature and V_{max} for human slow fibres has now been clearly demonstrated for a large population of rat fibres that

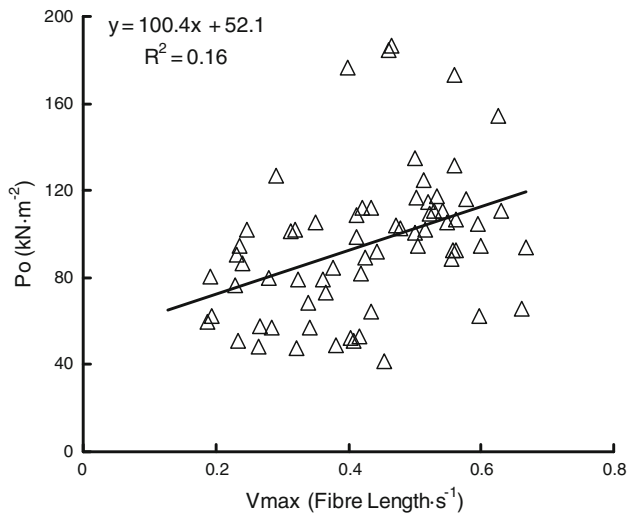


Fig. 10 Specific tension (P_o) as a function of maximum velocity of shortening (V_{max}) for individual single muscle fibres. V_{max} obtained by fitting force–velocity data to the Huxley model ($N = 68$)

are apparently all of the same type with respect of MHC and MLC composition. A simple kinetic analysis based on the Huxley model suggests that much of the variation in curvature of the force–velocity relationship is due to covariance of the rate constants f and g_2 . However, the variation in P_o that results from these kinetic differences explains only a small part of the variance in specific tension between fibres; the reason for the major part of this variance remains unknown.

Acknowledgments We appreciate the help of the technical staff of the animal houses at Manchester University and the Vrije Universiteit Amsterdam for the care of the animals.

References

- Andruchov O, Andruchova O, Wang Y, Galler S (2006) Dependence of cross-bridge kinetics on myosin light chain isoforms in rabbit and rat skeletal muscle fibres. *J Physiol* 571:231–242
- Bottinelli R, Schiaffino S, Reggiani C (1991) Force–velocity relations and myosin heavy chain isoform compositions of skinned fibres from rat skeletal muscle. *J Physiol* 437:655–672
- Bottinelli R, Betto R, Schiaffino S, Reggiani C (1994) Unloaded shortening velocity and myosin heavy chain and alkali light chain isoform composition in rat skeletal muscle fibres. *J Physiol* 478:341–349
- Bottinelli R, Canepari M, Pellegrino MA, Reggiani C (1996) Force–velocity properties of human skeletal muscle fibres: myosin heavy chain isoform and temperature dependence. *J Physiol* 495:573–586
- Burke RE, Levine DN, Zajac FE 3rd (1971) Mammalian motor units: physiological–histochemical correlation in three types in cat gastrocnemius. *Science* 174:709–712
- Burke RE, Levine DN, Tsairis P, Zajac FE (1973) Physiological types and histochemical profiles in motor units of the cat gastrocnemius. *J Physiol* 234:723–748

- Close RI (1972) Dynamic properties of mammalian skeletal muscles. *Physiol Rev* 52:129–197
- Degens H, Larsson L (2007) Application of skinned single muscle fibres to determine myofilament function in ageing and disease. *J Musculoskelet Neuronal Interact* 7:56–61
- Degens H, Yu F, Li X, Larsson L (1998) Effects of age and gender on shortening velocity and myosin isoforms in single rat muscle fibres. *Acta Physiol Scand* 163:33–40
- Degens H, Soop M, Hook P, Ljungqvist O, Larsson L (1999) Post-operative effects on insulin resistance and specific tension of single human skeletal muscle fibres. *Clin Sci (London, England: 1979)* 97:449–455
- Edman KA (2010) Contractile performance of striated muscle. *Adv Exp Med Biol* 682:7–40
- Edman KA, Reggiani C, te Kronnie G (1985) Differences in maximum velocity of shortening along single muscle fibres of the frog. *J Physiol* 365:147–163
- Edman KA, Mansson A, Caputo C (1997) The biphasic force–velocity relationship in frog muscle fibres and its evaluation in terms of cross-bridge function. *J Physiol* 503:141–156
- Frontera WR, Larsson L (1997) Contractile studies of single human skeletal muscle fibers: a comparison of different muscles, permeabilization procedures, and storage techniques. *Muscle Nerve* 20:948–952
- Gilliver SF, Degens H, Rittweger J, Sargeant AJ, Jones AD (2009) Variation in the determinants of power of chemically skinned human muscle fibres. *Exp Physiol* 94:1070–1078
- Greaser ML, Moss RL, Reiser PJ (1988) Variations in contractile properties of rabbit single muscle fibres in relation to troponin T isoforms and myosin light chains. *J Physiol* 406:85–98
- Hill AV (1938) The heat of shortening and the dynamic constants of muscle. *Proc R Soc Lond Ser B Biol Sci* 126:136–195
- Husom AD, Ferrington DA, Thompson LV (2005) Age-related differences in the adaptive potential of type I skeletal muscle fibers. *Exp Gerontol* 40:227–235
- Huxley AF (1957) Muscle structure and theories of contraction. *Progr Biophys Biophys Chem* 7:255–318
- Josephson RK, Edman KA (1988) The consequences of fibre heterogeneity on the force–velocity relation of skeletal muscle. *Acta Physiol Scand* 132:341–352
- Katz B (1939) The relation between force and speed in muscular contraction. *J Physiol* 96:45–64
- Lännergren J (1978) The force–velocity relation of isolated twitch and slow muscle fibres of *Xenopus laevis*. *J Physiol* 283:501–521
- Larsson L, Moss RL (1993) Maximum velocity of shortening in relation to myosin isoform composition in single fibres from human skeletal muscles. *J Physiol* 472:595–614
- Schiaffino S, Reggiani C (1996) Molecular diversity of myofibrillar proteins: gene regulation and functional significance. *Physiol Rev* 76:371–423
- Simmons RM, Jewell BR (1974) Mechanics and models of muscular contraction. In: Linden RJ (ed) Recent advances in physiology. Churchill Livingstone, London, pp 87–147
- Sweeney HL, Kushmerick MJ, Mabuchi K, Sréter FA, Gergely J (1988) Myosin alkali light chain and heavy chain variations correlate with altered shortening velocity of isolated skeletal muscle fibers. *J Biol Chem* 263:9034–9039
- Thompson LV, Brown M (1999) Age-related changes in contractile properties of single skeletal fibers from the soleus muscle. *J Appl Physiol* 86:881–886
- Wolledge RC, Curtin NA, Homsher E (1985) Energetic aspects of muscle contraction. *Monogr Physiol Soc* 41:1–357